AGU PUBLICATIONS

Geophysical Research Letters

RESEARCH LETTER
10.1002/2016GL069740

Key Points:
- Evidence of equatorial electrodynamics in launching poleward TIDs
- First simultaneous global observations of poleward and equatorward TIDs during storms
- Poleward TIDs mainly observed in the American and African sectors

Correspondence to:
J. B. Habarulema,
jhabarulema@sansa.org.za

Citation:
Habarulema, J. B., Z. T. Katamzi, E. Yizengaw, Y. Yamazaki, and G. Seemala (2016), Simultaneous storm time equatorward and poleward large-scale TIDs on a global scale, *Geophys. Res. Lett.*, *43*, 6678–6686, doi:10.1002/2016GL069740.

Received 22 APR 2016
Accepted 14 JUN 2016
Accepted article online 19 JUN 2016
Published online 2 JUL 2016

Simultaneous storm time equatorward and poleward large-scale TIDs on a global scale

John Bosco Habarulema[1,2], Zama Thobeka Katamzi[1,2], Endawoke Yizengaw[3], Yosuke Yamazaki[4], and Gopi Seemala[5]

[1]South African National Space Agency (SANSA) Space Science, Hermanus, South Africa, [2]Department of Physics and Electronics, Rhodes University, Grahamstown, South Africa, [3]Institute for Scientific Research, Boston College, Chestnut Hill, Massachusetts, USA, [4]Department of Physics, University of Lancaster, Lancaster, UK, [5]Indian Institute of Geomagnetism, Mumbai, India

Abstract We report on the first simultaneous observations of poleward and equatorward traveling ionospheric disturbances (TIDs) during the same geomagnetic storm period on a global scale. While poleward propagating TIDs originate from the geomagnetic equator region, equatorward propagating TIDs are launched from the auroral regions. On a global scale, we use total electron content observations from the Global Navigation Satellite Systems to show that these TIDs existed over South American, African, and Asian sectors. The American and African sectors exhibited predominantly strong poleward TIDs, while the Asian sector recorded mostly equatorward TIDs which crossed the geomagnetic equator to either hemisphere on 9 March 2012. However, both poleward and equatorward TIDs are simultaneously present in all three sectors. Using a combination of ground-based magnetometer observations and available low-latitude radar (JULIA) data, we have established and confirmed that poleward TIDs of geomagnetic equator origin are due to ionospheric electrodynamics, specifically changes in $\mathbf{E} \times \mathbf{B}$ vertical drift after the storm onset.

1. Introduction

Storm time investigations and analyses of large-scale traveling ionospheric disturbances (TIDs) are largely linked to storm-related phenomena that cause energy injected into auroral regions to launch gravity waves which are later manifested as equatorward traveling atmospheric disturbances. Since the earlier work linking atmospheric gravity waves to auroral region processes in storm time events [*Hines*, 1960], a number of numerical and observational studies exist and physical understanding about equatorward propagating TIDs (hereafter referred to as equatorward TIDs) and their characteristics is well established [e.g., *Balthazor and Moffett*, 1997; *Nicolls et al.*, 2004; *Borries et al.*, 2009; *Lei et al.*, 2008; *Ngwira et al.*, 2012; *Katamzi and Habarulema*, 2014, and references therein]. The conventional understanding has been that such equatorward disturbances can travel longer distances through midlatitudes crossing over to another hemisphere [see *Hajkowicz and Hunsucker*, 1987; *Balthazor and Moffett*, 1997; *Bruinsma and Forbes*, 2009; *Bowman and Mortimer*, 2011]. Literature about storm time poleward propagating TIDs (hereafter referred to as poleward TIDs) with no auroral origin is almost nonexistent. Only very recently, poleward results of large-scale TIDs were presented over China when the moderate storm that occurred in the period of 27 May to 1 June 2011 was in its recovery phase [*Ding et al.*, 2013]. *Ding et al.* [2013] suggested that energy dissipation from medium-scale TIDs of lower atmosphere origin can excite secondary large-scale TIDs that could propagate in the poleward direction, thus excluding the auroral regions as the primary source of such disturbances. Our focus in this paper is on poleward TIDs that have been found to be of geomagnetic equator origin during a geomagnetic storm condition on a global scale. Poleward TIDs possibly launched by equatorial electrojet were first suggested and shown numerically by *Chimonas* [1969] who investigated the strengths of such disturbances when the electrojet couples to the neutral atmosphere through Lorentz forcing. This mechanism involves transfer of force from ionized/charged to neutral particles through collisions thereby launching atmospheric gravity waves that result into TIDs. The first possible experimental evidence for such prediction was shown very recently [*Habarulema et al.*, 2015] over a region with sparse infrastructure network (African sector), which prompted the need to investigate their global characteristics. We have examined low to middle latitude global total electron content (TEC) changes on the 9 March 2012 storm to understand the characteristics of the associated TIDs and observed that their

direction is not consistent in the American, African, and Asian longitude sectors. Poleward TIDs were predominantly observed over South American and African sectors, while equatorward TIDs crossed the geomagnetic equator to either the Northern Hemisphere or Southern Hemisphere over the Asian sector. However, all the three sectors show simultaneous occurrence of both poleward and equatorward TIDs.

By utilizing ground-based magnetometer observations and 150 km drift echoes from Jicamarca Unattended Long-term studies of the Ionosphere and Atmosphere (JULIA) radar system, we have shown that the launching of poleward TIDs could be due to the low-latitude electrodynamics after the storm time onset and specifically the variability in vertical $\mathbf{E} \times \mathbf{B}$ ionospheric drift. To our knowledge, this is the first experimental study on a global scale showing the role of low-latitude electrodynamics in generating poleward TIDs of geomagnetic equator origin. In fact, poleward TIDs are very rarely reported in literature and our study suggests that this phenomena should be given attention in contributing to our understanding of global ionospheric response to geomagnetic storms.

2. Data Sources and Method

Both reported poleward and equatorward TID results on 9 March 2012 are based on observations from Global Navigation Satellite System (GNSS). A total of about 2500^+ GNSS receivers' data in receiver-independent exchange format was downloaded to derive slant TEC. The Boston College TEC derivation software/algorithm applied is similar to the one used in *Valladares et al.* [2009] and *Seemala and Valladares* [2011] and incorporates the slant to vertical TEC mapping technique that has its foundation described in a number of sources [*Leitinger et al.*, 1975; *Sardon et al.*, 1994; *Ciraolo and Spalla*, 1997]. Each satellite's time series of vertical TEC data was fitted with a polynomial (of fourth degree) over all receiver stations considered in order to estimate the ionospheric background TEC. This acted as the proxy of ionospheric TEC variability without storm-related influence. TEC was derived at a temporal resolution of 30 s. The difference between fitted and actual TEC then gave the detrended TEC (ΔTEC) called TEC perturbations. In simple terms, for each station, and for each satellite's time series vertical TEC, fitting was done as follows:

$$\begin{cases} vT^f(t)_{i,j} = at_{i,j}^4 + bt_{i,j}^3 + ct_{i,j}^2 + dt_{i,j} + \varepsilon, & \text{for} \quad j = 1, 2, \ldots, 31 \\ \Delta\text{TEC}(t)_{i,j} = \text{TEC}(t)_{i,j} - vT^f(t)_{i,j}, & \forall i, j \end{cases}$$

where $i = 1, 2, \ldots, 2500^+$ is the number of considered receiver stations; $j = 1, 2, \ldots, 31$ is the number of satellites; $vT^f(t)$ and $\text{TEC}(t)$ represent fitted and actual vertical TEC at time t; the coefficients a, b, c, d are obtained through the least squares method; and ε is the residual error of the fitting process. Final TEC consideration took into account an elevation threshold of 20° to minimize multipath effects. This is sufficient as individual ionospheric pierce points (IPPs) are considered for ΔTEC mapping and TIDs identification.

3. Results and Discussion

The month of March 2012 consisted of consecutive long duration disturbed events, and their interplanetary causes are described in details by *Tsurutani et al.* [2014]. The storm in our study occurred after the 7 March 2012 storm. Figure 1 shows changes in solar wind velocity (blue curve), IMF B_z (black curve), *SYM-H* index (black curve), and interplanetary electric field (IEF; $\text{IEF} = -v_x \times B_z$). The storm sudden commencement (SSC) occurred on 8 March 2012 (indicated by red dashed line) at 1103 UT, and the response is seen in solar wind velocity increase from about 490 to 780 m/s, while IMF B_z shortly turned northward. The main phase of the 9 March 2012 storm started nearly 13 h later after the SSC at 0100 UT and the *SYM-H* index's peak intensity was −148 nT at 0800 UT.

3.1. Global TEC Response

Figure 2 shows the variations of ΔTEC over American, African, and Asian sectors, within a range of 30° longitudes for each sector; and global ΔTEC maps from 1000 to 1100 UT at 20 min intervals. Figures 2a and 2b clearly show enhanced ΔTEC (in poleward direction) of geomagnetic equator origin. For example, this is clearly visible during 0600–0700 UT and 1000–1200 UT for both American and African sectors. Simultaneously, enhancement of ΔTEC in equatorward direction is present especially at around 0400 UT, 1000 UT, and 1400 UT over the southern hemispheric part of the African sector (see Figure 2b). From the available data, Figure 2a shows traces of equatorward TIDs in the Southern Hemisphere (see ~45°S–60°S) over the American sector at around 0600 UT and 0900 UT. An additional and distinct observation over the African sector is

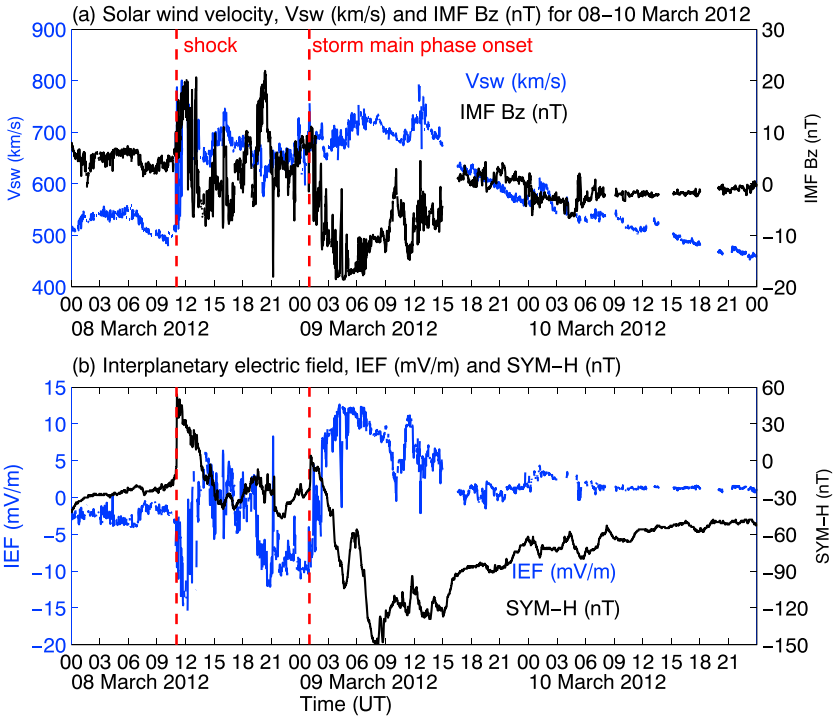

Figure 1. Variations of solar wind velocity, B_z component of the interplanetary magnetic field IMF B_z (nT), *SYM-H* (nT), and interplanetary electric field, IEF (mV/m) for 8–10 March 2012. Vertical red dashed lines represent shock time (11:03 UT on 8 March 2012) and storm time main phase onset (0100 UT on 9 March 2012), respectively. A 1 min solar wind data shifted to the Earth's bow shock nose were used.

the instantaneous enhancement of TEC at all latitudes at about 0100–0300 UT which is typical response of the ionospheric electron density to prompt penetration electric field as we will discuss later in the next subsection. For the Asian sector (Figure 2c), the dominant observation is the enhanced ΔTEC across the equator from either hemisphere. Signatures of equatorward propagation are clear over the Asian sector where TIDs from the Northern and Southern Hemispheres appear to meet at the geomagnetic equator and crossover to either hemisphere just before 0400 UT and at around 1400 UT. Figure 2d shows horizontal extracts of ΔTEC at different geographic latitudes over the American, African, and Asian sectors, respectively. Although there is generally little data in the Northern Hemisphere's parts over the American and African sectors within our considered spatial resolution, clear poleward propagation is visible in both cases. Over the Asian sector, equatorward TIDs are mostly from the Southern Hemisphere to Northern Hemisphere. Figures 2e–2h show global ΔTEC maps generated by binning ΔTEC data within a spatial resolution of 2.5° × 4° in latitude and longitude, from 1000 to 1100 UT. From the Northern Hemisphere, an equatorward TID front can be seen in the American sector (see its south-east motion within ~45°N–75°N and ~170°W–100°W, from 1000 to 1100 UT). Within the same time interval, the poleward TID from around the geomagnetic equator has moved to the EIA crest by 1100 UT (Figure 2h) in the southern hemispheric part of the American sector. Northern Hemisphere poleward TID is visible but not as clear as the Southern Hemisphere TID propagation, because of its north-east direction over the ocean area that does not have data. This case in point illustrates that equatorward and poleward TIDs are simultaneously present during one storm period. Assuming perfect poleward/equatorward propagation virtual velocities of the TIDs calculated from time lags between TEC peak occurrences [e.g., *Ngwira et al.*, 2012; *Katamzi and Habarulema*, 2014] using BRAZ (15.95°S, 47.88°W), GOJA (17.88°S, 51.73°W), and SPAR (21.18°S, 50.44°W), GNSS receiver stations (in Brazil) reach about 678 ± 62 m/s along 50°W longitude (e.g., at ~1614–1633 UT). Along the 103°E longitude, the computed virtual velocity based on XMIS, Australia, (10.45°S, 105.69°E); NTUS, Singapore, (1.35°N, 103.68°E); and CUSV, Thailand, (13.74°N, 100.53°E) receiver stations is 495 ± 126 m/s during 0748–0920 UT. We note that the true phase velocities of the associated TIDs when their actual directions are taken into account are usually lower than the apparent/virtual values (which assume exact equatorward/poleward direction) reported here [e.g., *Habarulema et al.*, 2013, 2015, and references therein].

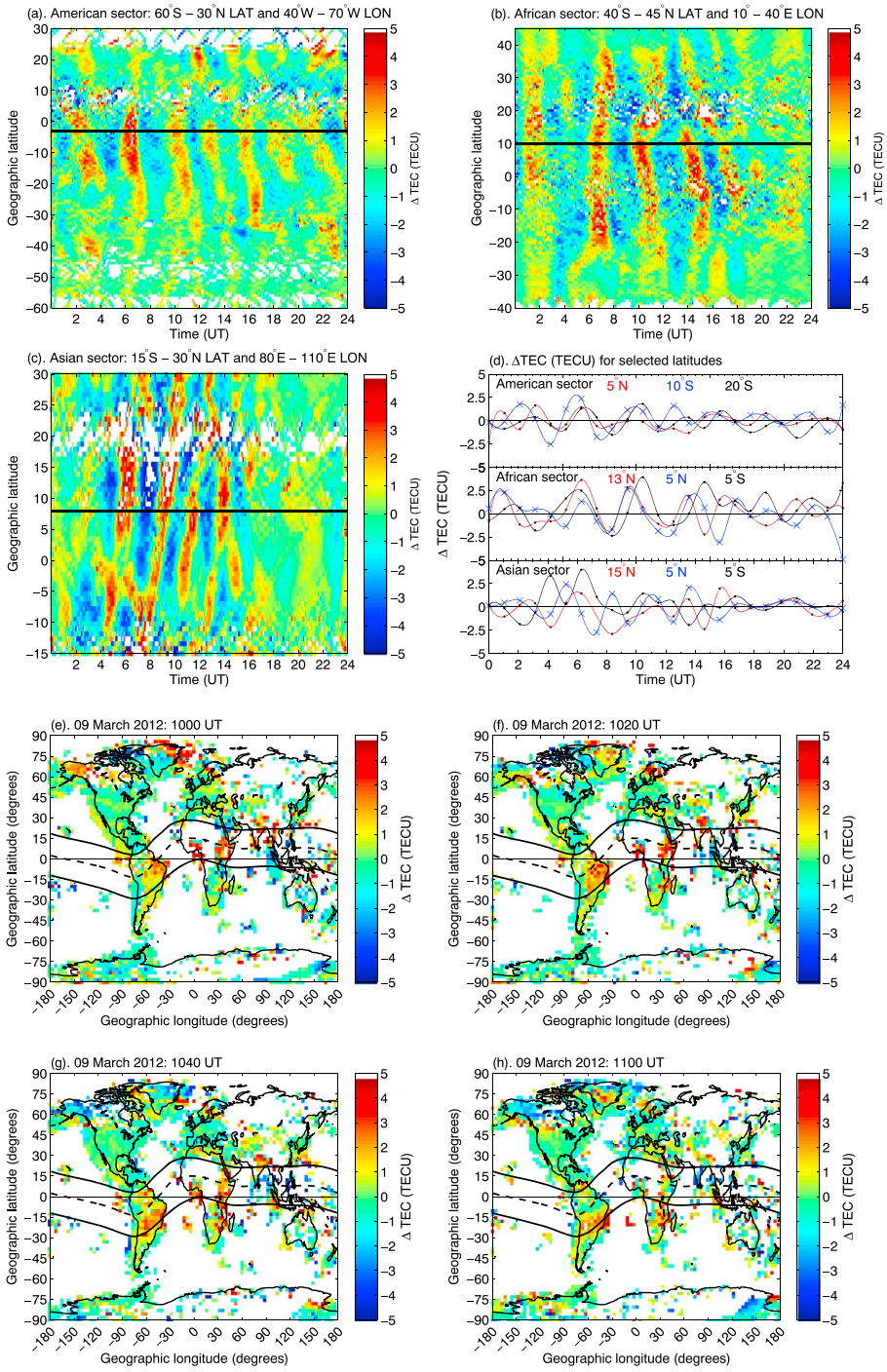

Figure 2. TEC perturbations, ΔTEC (TECU) for (a) American, (b) African, and (c) Asian sectors on 9 March 2012. Black solid lines in Figures 2a–2c approximate the geomagnetic equator in the three sectors. ΔTEC and latitudes were binned at 3 min and 0.8°, respectively. (d) ΔTEC (TECU) averaged in 1 h bins for selected latitudes in the three longitude sectors where a marker cross is used on the blue curve for clarity. (e)–(h) Global two-dimensional ΔTEC maps (spatial resolution of 2.5° × 4° in latitude and longitude) from 1000 to 1100 UT in 20 min intervals.

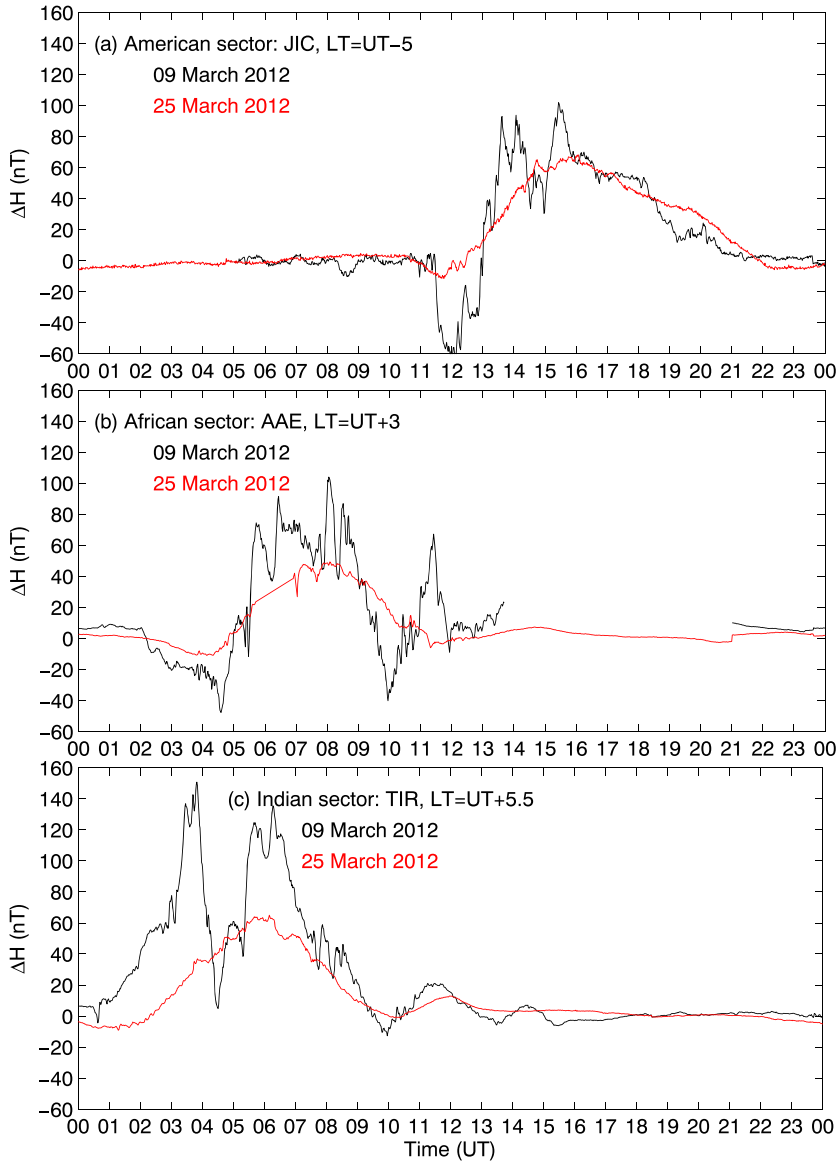

Figure 3. Variations of ΔH ($\propto \mathbf{E} \times \mathbf{B}$ drift) derived from differential magnetometer approach over the American, African, and Indian sectors for the disturbed (9 March 2012) and quiet (25 March 2012) conditions.

3.2. Observations and Possible Driving Mechanisms

Figure 3 shows changes of ΔH (which has a linear relationship with $\mathbf{E} \times \mathbf{B}$ drift velocities during local daytime) values derived from differential magnetometer approach [*Rastogi and Klobuchar*, 1990; *Anderson et al.*, 2004; *Yizengaw et al.*, 2011, 2012, 2014] over the American, African, and Indian sectors for the disturbed (9 March 2012) and quiet (25 March 2012) conditions, respectively. A link between the equatorial electrojet and vertical $\mathbf{E} \times \mathbf{B}$ drift was quantitatively established by *Anderson et al.* [2002]. Following this, *Anderson et al.* [2004] derived an empirical relationship between $\mathbf{E} \times \mathbf{B}$ and daytime equatorial electrojet that has proved to work in different longitude sectors as validated with different data sources [see *Yizengaw et al.*, 2011, 2014, and references therein]. For the three sectors, Table 1 shows the geographic and geomagnetic locations of magnetometer stations which were used for vertical drift inference on both quiet and disturbed days. In the Africa sector, Adigrat (ETHI) (14. 3°N, 39.5°E) belongs to the African Meridian and B-Field Education Research (AMBER) network [*Yizengaw and Moldwin*, 2009], while Addis Ababa (AAE) (9.0°N, 38.8°E) is part of the International Magnetic Network (INTERMAGNET) observatories. Both Piura (PIU) (5.2°S, 80.6°W) and Jicamarca (JIC) (11.8°S, 77.2°W) are operated and owned by the Jicamarca Radio Observatory (JRO). Tirunelveli (TIR) (8.7°N, 77.7°E) belongs to the Indian Institute of Geomagnetism (IIG), while Alibag (ABG) (18.64°N, 72.87°E) is an INTERMAGNET

Table 1. Pairs of Geomagnetic Stations Used to Estimate **E** × **B** Vertical Velocities Over the American, African, and Indian Sectors

			Geographic Coordinates		Geomagnetic Coordinates	
Station	Code	Ownership	Latitude	Longitude	Latitude	Longitude
American Sector						
Jicamarca	JIC	JRO	−11.8	−77.2	0.8	−5.7
Piura	PIU	JRO	−5.2	−80.6	6.8	−9.4
African Sector						
Adigrat	ETHI	AMBER	14.3	39.5	6.0	111.1
Addis Ababa	AAE	INTERMAGNET	9.0	38.8	0.2	110.5
Indian Sector						
Tirunelveli	TIR	IIG	8.7	77.7	0.6	149.5
Alibag	ABG	INTERMAGNET	18.6	72.9	11.8	145.1

station. The 25 March 2012 served the purpose of the quiet period reference for assessing **E** × **B** response due to increased geomagnetic activity. In the American sector (JIC), see (Figure 3a), there is a decrease of ΔH which indicates a westward **E** × **B** between 1100 and 1300 UT (0600–0800 LT) and after this time ΔH starts a gradual increase. As this includes local daytime, one would expect an increase starting at sunrise in a relatively similar trend as for 25 March 2012. Therefore, the storm-related dynamics led to the sharp decrease in ΔH (**E** × **B**). Storm time low-latitude electrodynamics are influenced mainly by direct/prompt penetration electric fields, PPEFs, [*Nishida*, 1968] and disturbance dynamo electric fields [*Blanc and Richmond*, 1980]. PPEFs cause **E** × **B** increase during daytime and a decrease at nighttime [*Fejer and Scherliess*, 1995, 1998], while disturbance dynamo electric field causes decrease and increase in daytime and nighttime **E** × **B** vertical drift, respectively [see *Blanc and Richmond*, 1980; *Fejer and Scherliess*, 1995; *Huang*, 2013, and references therein]. The observed ΔH decrease almost 10 h after the commencement of the main phase makes disturbance dynamo effect a possible contributor to the westward electric field during 1100–1300 UT (0600–0800 LT). Numerical and observational investigations have indicated that the disturbance dynamo electric field can last hours to a day after the ceasing of high-latitude activity/maximum geomagnetic activity [*Huang et al.*, 2005; *Yamazaki and Kosch*, 2015]. The downward vertical drift observed in magnetometer data (Figure 3a) between 1100 and 1300 UT (0600–0800 LT) agrees well with the decrease in TEC as shown in Figure 2a. It is a difficult task to relate ΔH variability to observed TID signatures in Figure 2a at 0200 UT, 0600 UT, and 1000 UT as this is local nighttime over JIC and magnetometer observations are a reliable electrodynamics indicator only during daytime. There should be a source of eastward electric field leading to enhanced vertical drifts which could later drive the observed TIDs. Between ~0200 and 0300 UT, Figure 2a shows increased TEC at almost all latitudes, although there are some data gaps. A similar case exists over the African sector and will be discussed later. Figure 4 shows ΔTEC over South American sector and the 150 km drift echoes from JULIA system along with ΔH values over Jicamarca on 9 March 2012. It has been previously shown that JULIA daytime vertical velocities agree well with *F* region incoherent scatter radar observations [*Chau and Woodman*, 2004], and JULIA data are therefore a reliable data set to provide a picture of the local time electrodynamics over Jicamarca during the period under consideration. Figure 4b shows that the increase in JULIA vertical drift reaching 25 m/s at 1552 UT coincided with observation of poleward TIDs. Peak occurrence in JULIA vertical drift is in agreement with JIC ΔH data. JULIA vertical drift starts decreasing until 1708 UT (1208 LT) when a corresponding depletion in TEC is observed over the South American sector. JULIA vertical drift increased, reached a peak of 18 m/s at 1818 UT (1318 LT), and at the same time clear TID signatures from the geomagnetic equator are again observed. It is evident that the dynamics of these disturbances are clearly associated with the changes in **E** × **B** vertical drift fluctuations. JULIA results therefore confirm that these ionospheric disturbances of geomagnetic equator origin are directly related to low-latitude electrodynamics through Lorentz coupling. Although there may be other factors contributing to low-latitude electrodynamics, it is expected that low-latitude/equatorial latitude ΔTEC peaks will not directly match ΔH during daytime mainly because of the local time effect in our analysis. While ΔH is computed at one longitude location, ΔTEC values shown in Figures 2a–2d are a combination of ionospheric TEC changes within a 30° longitude sector translating into a local time difference of about 2 h between the lower and upper limit longitude values in each sector.

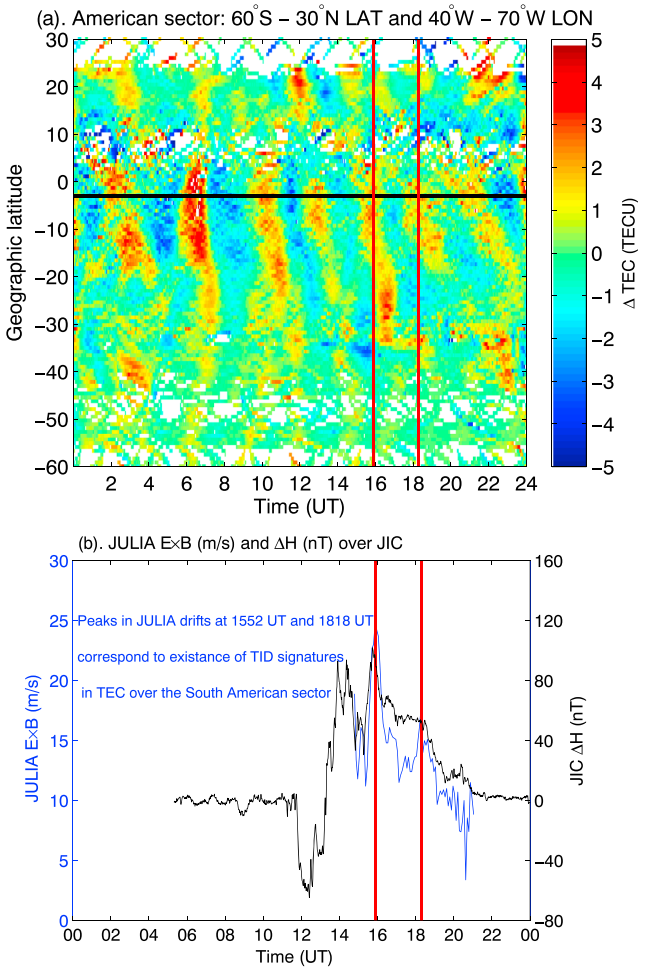

Figure 4. Diurnal variations of (a) ΔTEC over the American sector and (b) JULIA 150 km drift echoes and ΔH values for Jicamarca, JIC, on 9 March 2012. The enhancement and subsequent appearance of peaks in JULIA data (represented by red solid lines) correspond to the existence of TID signatures from TEC at ~1552 UT and ~1818 UT, respectively. JIC ΔH and JULIA $\mathbf{E} \times \mathbf{B}$ drift data have temporal resolutions of 1 and 5 min, respectively.

First observational results showing possible poleward TIDs were first reported by *Habarulema et al.* [2015] over the African sector putting forward the dynamics of equatorial electrojet (EEJ) as the primary mechanism through Lorentz forcing. We wish to restate that possibilities of EEJ's role in driving poleward TIDS were first suggested and numerically shown by *Chimonas* [1969]. We notice the simultaneous increase in TEC over all latitudes in the African sector (see Figure 2b) during 0100–0300 UT which is not captured by ΔH (see Figure 3b) as the currents are too weak to be detected by the magnetometer during nighttime. Prior to the 9 March 2012 storm, a shock hit the magnetosphere at ~11:03 UT on 8 March 2012 (after the 7 March 2012 storm). The IEF values increased significantly due to the increased solar wind velocities associated with this storm [*Tsurutani et al.*, 2014]. The high IEF values could then directly end up in the magnetosphere-ionosphere system and penetrate to middle and low/equatorial latitudes. *Sastri* [2002] studied the nighttime response of the zonal electric field (at equatorial latitudes) to the preliminary impulse of sudden storm commencement of 8 July 1991 and reported the instantaneous transfer of the associated polar electric field to dip equator on the nightside. He showed that eastward electric field can grow and decay during nighttime at the dip equator/low latitudes within an hour after the sudden storm commencement which seems consistent with simultaneous TEC enhancement over the African sector starting from 0100 UT, the storm main phase onset time. The nighttime eastward electric field was explained to be due to the dawn-dusk electric field penetration related to the R1 field aligned currents' enhancement of the solar wind origin [*Sastri*, 2002], and this could be the cause of the

simultaneous TEC enhancement between 0100 and 0200 UT (Figure 2b) over the African sector. The decrease of ΔH after sunrise (2 h after the storm main phase onset) is because of the disturbance dynamo electric field contribution to low-latitude ionospheric drifts. At around 0600 UT (0900 LT), an enhancement or launching of TIDs from the equator is seen in Figure 2b and this corresponded to increased ΔH. The other group of TIDs is launched at about 0900 UT (1200 LT); thereafter, a decrease in ΔH is observed which corresponds to TEC depletion. Another significant TID signature is observed just before 1400 UT (1700 LT). Specifically over the African sector, clear equatorward TIDs of auroral origin are observed which get dominated by poleward TIDs at about 20°S latitude. The reported poleward TIDs in Figures 2a and 2b can propagate a distance of about 20°–30° (~2200 km–3300 km) from their point of origin.

Figure 3c shows ΔH variations over the Indian sector used as a proxy to understand local electrodynamics in the Asian sector. TEC dynamics over the Asian sector was in some aspects different from South American and African sectors' results. Starting at about 0200 UT in Figure 2c, there is an observation of poleward propagation in both hemispheres reaching about 10° from the magnetic equator. During this time, ΔH ($\mathbf{E}\times\mathbf{B}$ vertical drift) was on a gradual increase. At about 0430 UT, there is an interference between poleward and equatorward propagation at 2°S geographic, with the latter appearing to dominate. It is noticed that ΔH started decreasing sharply just before 0430 UT (1000 LT; Figure 3c). There after, all significant TID signatures (e.g., between 0400–0500 UT, 0700–0800 UT, and 1000–1100 UT, respectively) appear to be equatorward crossing from the Southern Hemisphere to Northern Hemisphere as shown in Figure 2c with exception of two TIDs which met at the equator from both hemispheres at around 1400 UT. According to observations from ~0200 to 0430 UT, electrodynamics would therefore seem to suggest that when there is a strong decrease in ΔH (downward $\mathbf{E}\times\mathbf{B}$) at the geomagnetic equator, equatorward TIDs dominate poleward TIDs. However, ΔH was mostly positive between ~0500 and 1400 UT when equatorward TIDs were dominant over the Asian sector. This implies that strong vertical drift did not significantly contribute to poleward TIDs in this sector. From this analysis, it is not clear why equatorward TIDs are more dominant in the Asian sector, while poleward TIDs possibly launched from the equatorial region dominate within the American and African sectors. More investigations are required to understand this, especially on the establishment of long-term occurrence of poleward TIDs.

4. Summary

This paper presented simultaneous observations of poleward and equatorward TIDs for 9 March 2012 storm on a global scale. We found that poleward TIDs originating from the geomagnetic equator dominated over the South American and African sectors, while equatorward TIDs propagated and crossed over to either the Northern Hemisphere or Southern Hemisphere for the Asian sector. In all the three sectors, traces of equatorward TIDs were evident. It is difficult to isolate the dominant physical mechanism for each observation as the ionosphere and thermosphere are under the influence of both internal and external dynamical and electrodynamical sources such as magnetospheric and disturbance dynamo electric field contributions as well as global changes in thermospheric neutral wind. Electric fields related to both prompt penetration and disturbance dynamo could have dominated processes leading to poleward TIDs over the American and African sectors. Storm time disturbed neutral winds contributed to equatorward TIDs [*Hocke and Schlegel*, 1996] which were predominantly observed over the Asian sector. In the past, literature about poleward TIDs mainly reported on interhemispherical crossover to different hemispheres [*Hajkowicz and Hunsucker*, 1987; *Balthazor and Moffett*, 1997; *Bruinsma and Forbes*, 2009; *Bowman and Mortimer*, 2011]. TIDs originating from the geomagnetic equator during storms have been rarely reported, despite having been suggested and numerically shown by *Chimonas* [1969]. A link to direct observational evidence of poleward TIDs was recently presented in a region with sparse instrumentation over the low-latitude region [*Habarulema et al.*, 2015]. In this paper, we have shown that such poleward TIDs were present on a global scale by looking at a combination of American, African, and Asian sectors. Through Lorentz coupling of the electrojet with neutral atmosphere which gets enhanced during geomagnetic storms, we have established and confirmed that local electrodynamics are responsible for poleward TIDs that originate from the geomagnetic equator. The JULIA 150 km echo data were instrumental in confirming this along with ground-based magnetometer observations. Our results suggest that disturbances of geomagnetic equator origin should be given attention as they will contribute to our understanding of global ionospheric response to geomagnetic storms. In this regard, a comprehensive climatological study is suggested to establish the trends of occurrence of poleward TIDs during geomagnetic storm conditions.

Acknowledgments
GNSS data were obtained from African Reference Frame, AFREF (ftp://ftp.afrefdata.org); IGS (ftp://garner.ucsd.edu); University Navstar Consortium, UNAVCO (ftp://data-out.unavco.org); the South African National Geospatial Information (ftp://ftp.trignet.co.za); and the Brazilian Network for Continuous GPS Monitoring, RBMC (ftp://geoftp.ibge.gov.br/RBMC/dados/). JULIA was obtained from jro.igp.gob.pe. Data for solar wind parameters are available from the web omniweb.gsfc.nasa.gov. This research is supported by the South African National Research Foundation grants 84240 and 90331. Different national institutes which support collected geomagnetic data are acknowledged. Thanks to INTERMAGNET for promoting high standards of magnetic observatory practice. NSF (AGS145136) and AFOSR (FA9550-12-1-0437 and FA9550-15-1-0399) grants partially supported E.Y.'s contribution.

References

Anderson, D., A. Anghel, K. Yumoto, M. Ishitsuka, and E. Kudeki (2002), Estimating daytime vertical E × B drift velocities in the equatorial F-region using ground-based magnetometer observations, *Geophys. Res. Lett.*, *29*(12), 1596, doi:10.1029/2001GL014562.

Anderson, D., A. Anghel, J. Chau, and O. Veliz (2004), Daytime E × B drift velocities inferred from ground-based magnetometers at low latitudes, *Space Weather*, *2*, S11001, doi:10.1029/2004SW000095.

Balthazor, R. L., and R. J. Moffett (1997), A study of atmospheric gravity waves and travelling ionospheric disturbances at equatorial latitudes, *Ann. Geophys.*, *15*, 1048–1056.

Bowman, G. G., and I. K. Mortimer (2011), Some aspects of large-scale travelling ionospheric disturbances which originate at conjugate locations in auroral zones, cross the equator and sometimes encircle the Earth, *Ann. Geophys.*, *29*, 2203–2210.

Borries, C., N. Jakowski, and V. Wilken (2009), Storm induced large scale TIDs observed in GPS derived TEC, *Ann. Geophys.*, *27*, 1605–1612.

Blanc, M., and A. D. Richmond (1980), The ionospheric disturbance dynamo, *J. Geophys. Res.*, *85*, 1669–1686.

Bruinsma, S. L., and J. M. Forbes (2009), Properties of traveling atmospheric disturbances (TADs) inferred from CHAMP accelerometer observations, *Adv. Space Res.*, *43*, 369–376.

Chau, J. L., and R. F. Woodman (2004), Daytime vertical and zonal velocities from 150-km echoes: Their relevance to F-region dynamics, *Geophys. Res. Lett.*, *31*, L17801, doi:10.1029/2004GL020800.

Chimonas, G (1969), The upper atmosphere in motion: The equatorial electrojet as a source of long period travelling ionospheric disturbances, *Geophys. Monogr. Ser.*, *18*, 698–706.

Ciraolo, L., and P. Spalla (1997), Comparison of ionospheric total electron content from the navy navigation satellite system and the GPS, *Radio Sci.*, *32*(3), 1071–1080.

Ding, F., W. Wan, B. Ning, B. Zhao, Q. Lin, Y. Wang, L. Hu, R. Zhang, and B. Xiong (2013), Observations of poleward-propagating large-scale traveling ionospheric disturbances in Southern China, *Ann. Geophys.*, *31*, 377–385.

Fejer, B. G., and L. Scherliess (1995), Time dependent response of equatorial ionospheric electric field to magnetospheric disturbances, *Geophys. Res. Lett.*, *22*(7), 851–854.

Fejer, B. G., and L. Scherliess (1998), Mid- and low-latitude prompt ionospheric zonal plasma drifts, *Geophys. Res. Lett.*, *25*(16), 3071–3074.

Habarulema, J. B., Z. T. Katamzi, and L.-A. McKinnell (2013), Estimating the propagation characteristics of large-scale TIDs using ground-based and satellite data, *J. Geophys. Res. Space Phys.*, *118*, 7768–7782, doi:10.1002/2013JA018997.

Habarulema, J. B., Z. T. Katamzi, and E. Yizengaw (2015), First observations of poleward large-scale traveling ionospheric disturbances over the African sector during geomagnetic storm conditions, *J. Geophys. Res. Space Phys.*, *120*, 6914–6929, doi:10.1002/2015JA021066.

Hajkowicz, L. A., and R. D. Hunsucker (1987), A simultaneous observation of large-scale periodic TIDs in both hemispheres following an onset of auroral disturbances, *Planet. Space Sci.*, *35*(6), 785–791.

Hines, C. O. (1960), Internal atmospheric gravity waves at ionospheric heights, *Can. J. Phys.*, *38*(11), 1441–1481.

Hocke, K., and K. Schlegel (1996), A review of atmospheric gravity waves and travelling ionospheric disturbances, *Ann. Geophys.*, *14*, 917–940.

Huang, C. M. (2013), Disturbance dynamo electric fields in response to geomagnetic storms occurring at different universal times, *J. Geophys. Res.*, *118*, 496–501, doi:10.1029/2012JA018118.

Huang, C. M., A. D. Richmond, and M.-Q. Chen (2005), Theoretical effects of geomagnetic activity on low-latitude electric fields, *J. Geophys. Res.*, *110*, A05312, doi:10.1029/2004JA010994.

Katamzi, Z. T., and J. B. Habarulema (2014), Traveling ionospheric disturbances observed at South African midlatitudes during the 29–31 October 2003 geomagnetically disturbed period, *Adv. Space Res.*, *53*(1), 48–62.

Lei, J., A. G. Burns, T. Tsugawa, S. C. Solomon, and M. Wiltberger (2008), Observations and simulations of quasiperiodic oscillations and large-scale travelling ionospheric disturbances during the December 2006 geomagnetic storm, *J. Geophys. Res.*, *113*, A06310, doi:10.1029/2007JA013090.

Leitinger, R., G. Schmidt, and A. Tauriainen (1975), An evaluation method combining the differential Doppler measurements from two stations that enables the calculation of the electron content of the ionosphere, *J. Geophys.*, *41*(2), 201–213.

Nicolls, M. J., M. C. Kelley, A. J. Coster, S. A. González, and J. Makela (2004), Imaging the structure of a large-scale TID using ISR and TEC data, *Geophys. Res. Lett.*, *31*, L09812, doi:10.1029/2004GL019797.

Ngwira, C. M., L.-A. McKinnell, P. J. Cilliers, and E. Yizengaw (2012), An investigation of ionospheric disturbances over South Africa during the magnetic storm on 15 May 2005, *Adv. Space Res.*, *49*, 327–335.

Nishida, A. (1968), Coherence of DP 2 fluctuations with interplanetary magnetic field variations, *J. Geophys. Res.*, *73*, 5549–5559.

Rastogi, R. G., and J. A. Klobuchar (1990), Ionospheric electron content within the equatorial F_2 layer anomaly belt, *J. Geophys. Res.*, *95*(A11), 19,045–19,052.

Sardon, E., A. Rius, and N. Zarraoa (1994), Estimation of the transmitter and receiver differential biases and the ionospheric total electron content from Global Positioning System observations, *Radio Sci.*, *29*(3), 577–586.

Sastri, J. H. (2002), Penetration electric fields at the nightside dip equator associated with the main impulse of the storm sudden commencement of 8 July 1991, *J. Geophys. Res.*, *107*(A12), 1448, doi:10.1029/2002JA009453.

Seemala, G. K., and C. E. Valladares (2011), Statistics of total electron content depletions observed over the South American continent for the year 2008, *Radio Sci.*, *46*, RS5019, doi:10.1029/2011RS004722.

Tsurutani, B. T., E. Echer, K. Shibata, O. P. Verkhoglyadova, A. J. Mannucci, W. D. Gonzalez, J. U. Kozyra, and M. Patzold (2014), The interplanetary causes of geomagnetic activity during the 7–17 March 2012 interval: A CAWSES II overview, *J. Space Weather Space Clim.*, *4*(A02), A02p1–A02p7, doi:10.1051/swsc/2013056.

Valladares, C. E., J. Villalobos, M. A. Hei, R. Sheehan, S. Basu, E. MacKenzie, P. H. Doherty, and V. H. Rios (2009), Simultaneous observation of travelling ionospheric disturbances in the Northern and Southern Hemispheres, *Ann. Geophys.*, *27*, 1501–1508.

Yamazaki, Y., and M. J. Kosch (2015), The equatorial electrojet during geomagnetic storms and substorms, *J. Geophys. Res. Space Physics*, *120*, 2276–2287, doi:10.1002/2014JA020773.

Yizengaw, E., and M. B. Moldwin (2009), African Meridian B-field Education and Research (AMBER) array, *Earth Moon Planet*, *104*, 237–246, doi:10.1007/s11038-008-9287-2.

Yizengaw, E., M. B. Moldwin, A. Mebrahtu, B. Damtie, E. Zesta, C. E.Valladares, and P. H. Doherty (2011), Comparison of storm time equatorial ionospheric electrodynamics in the African and American sectors, *J. Atmos. Sol. Terr. Phys.*, *73*(1), 156–163.

Yizengaw, E., E. Zesta, M. B. Moldwin, B. Damtie, A. Mebrahtu, C. E. Valladares, and R. F. Pfaff (2012), Longitudinal differences of ionospheric vertical density distribution and equatorial electrodynamics, *J. Geophys. Res.*, *A07312*, doi:10.1029/2011JA017454.

Yizengaw, E., M. B. Moldwin, E. Zesta, C. M. Biouele, B. Damtie, A. Mebrahtu, B. Rabiu, C. E. Valladares, and R. Stoneback (2014), The longitudinal variability of equatorial electrojet and vertical drift velocity in the African and American sectors, *Ann. Geophys.*, *32*, 231–238.